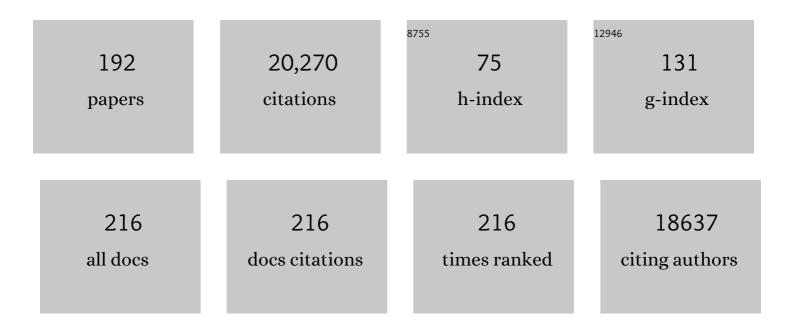
Nikolaus Weiskopf

List of Publications by Year in descending order

Source: https://exaly.com/author-pdf/114431/publications.pdf Version: 2024-02-01



#	Article	IF	CITATIONS
1	Closed-loop brain training: the science of neurofeedback. Nature Reviews Neuroscience, 2017, 18, 86-100.	10.2	814
2	When Fear Is Near: Threat Imminence Elicits Prefrontal-Periaqueductal Gray Shifts in Humans. Science, 2007, 317, 1079-1083.	12.6	798
3	A comparison between voxel-based cortical thickness and voxel-based morphometry in normal aging. Neurolmage, 2009, 48, 371-380.	4.2	504
4	Context-Dependent Human Extinction Memory Is Mediated by a Ventromedial Prefrontal and Hippocampal Network. Journal of Neuroscience, 2006, 26, 9503-9511.	3.6	464
5	Evidence of Mirror Neurons in Human Inferior Frontal Gyrus. Journal of Neuroscience, 2009, 29, 10153-10159.	3.6	459
6	Comparing hemodynamic models with DCM. NeuroImage, 2007, 38, 387-401.	4.2	449
7	Optimal EPI parameters for reduction of susceptibility-induced BOLD sensitivity losses: A whole-brain analysis at 3ÅT and 1.5ÅT. NeuroImage, 2006, 33, 493-504.	4.2	444
8	Quantitative multi-parameter mapping of R1, PD*, MT, and R2* at 3T: a multi-center validation. Frontiers in Neuroscience, 2013, 7, 95.	2.8	428
9	Adolescence is associated with genomically patterned consolidation of the hubs of the human brain connectome. Proceedings of the National Academy of Sciences of the United States of America, 2016, 113, 9105-9110.	7.1	415
10	Real-time fMRI neurofeedback: Progress and challenges. NeuroImage, 2013, 76, 386-399.	4.2	398
11	Physiological self-regulation of regional brain activity using real-time functional magnetic resonance imaging (fMRI): methodology and exemplary data. NeuroImage, 2003, 19, 577-586.	4.2	375
12	Principles of a Brain-Computer Interface (BCI) Based on Real-Time Functional Magnetic Resonance Imaging (fMRI). IEEE Transactions on Biomedical Engineering, 2004, 51, 966-970.	4.2	366
13	Regulation of emotional responses elicited by threat-related stimuli. Human Brain Mapping, 2007, 28, 409-423.	3.6	362
14	Regulation of anterior insular cortex activity using real-time fMRI. NeuroImage, 2007, 35, 1238-1246.	4.2	322
15	Threatening a rubber hand that you feel is yours elicits a cortical anxiety response. Proceedings of the National Academy of Sciences of the United States of America, 2007, 104, 9828-9833.	7.1	312
16	Using high-resolution quantitative mapping of R1 as an index of cortical myelination. NeuroImage, 2014, 93, 176-188.	4.2	299
17	Distinct Causal Influences of Parietal Versus Frontal Areas on Human Visual Cortex: Evidence from Concurrent TMS-fMRI. Cerebral Cortex, 2008, 18, 817-827.	2.9	282
18	Anterolateral Prefrontal Cortex Mediates the Analgesic Effect of Expected and Perceived Control over Pain. Journal of Neuroscience, 2006, 26, 11501-11509.	3.6	276

#	Article	IF	CITATIONS
19	Real-time fMRI and its application to neurofeedback. NeuroImage, 2012, 62, 682-692.	4.2	261
20	Regional specificity of MRI contrast parameter changes in normal ageing revealed by voxel-based quantification (VBQ). NeuroImage, 2011, 55, 1423-1434.	4.2	259
21	Widespread age-related differences in the human brain microstructure revealed by quantitative magnetic resonance imaging. Neurobiology of Aging, 2014, 35, 1862-1872.	3.1	248
22	MRI investigation of the sensorimotor cortex and the corticospinal tract after acute spinal cord injury: a prospective longitudinal study. Lancet Neurology, The, 2013, 12, 873-881.	10.2	239
23	Disability, atrophy and cortical reorganization following spinal cord injury. Brain, 2011, 134, 1610-1622.	7.6	238
24	Mapping the Human Cortical Surface by Combining Quantitative T1 with Retinotopyâ€. Cerebral Cortex, 2013, 23, 2261-2268.	2.9	236
25	Flow of affective information between communicating brains. NeuroImage, 2011, 54, 439-446.	4.2	234
26	Apparent thinning of human visual cortex during childhood is associated with myelination. Proceedings of the National Academy of Sciences of the United States of America, 2019, 116, 20750-20759.	7.1	231
27	Self-regulation of local brain activity using real-time functional magnetic resonance imaging (fMRI). Journal of Physiology (Paris), 2004, 98, 357-373.	2.1	226
28	Real-time functional magnetic resonance imaging: methods and applications. Magnetic Resonance Imaging, 2007, 25, 989-1003.	1.8	224
29	Selfâ€regulation of regional cortical activity using realâ€time fMRI: The right inferior frontal gyrus and linguistic processing. Human Brain Mapping, 2009, 30, 1605-1614.	3.6	219
30	Locus coeruleus imaging as a biomarker for noradrenergic dysfunction in neurodegenerative diseases. Brain, 2019, 142, 2558-2571.	7.6	219
31	<i>In Vivo</i> Functional and Myeloarchitectonic Mapping of Human Primary Auditory Areas. Journal of Neuroscience, 2012, 32, 16095-16105.	3.6	206
32	The impact of physiological noise correction on fMRI at 7 T. NeuroImage, 2011, 57, 101-112.	4.2	199
33	Mapping causal interregional influences with concurrent TMS–fMRI. Experimental Brain Research, 2008, 191, 383-402.	1.5	197
34	Decoding Neuronal Ensembles in the Human Hippocampus. Current Biology, 2009, 19, 546-554.	3.9	197
35	Detecting Representations of Recent and Remote Autobiographical Memories in vmPFC and Hippocampus. Journal of Neuroscience, 2012, 32, 16982-16991.	3.6	191
36	The Role of Contralesional Dorsal Premotor Cortex after Stroke as Studied with Concurrent TMS-fMRI. Journal of Neuroscience, 2010, 30, 11926-11937.	3.6	190

#	Article	IF	CITATIONS
37	Decoding Individual Episodic Memory Traces in the Human Hippocampus. Current Biology, 2010, 20, 544-547.	3.9	187
38	Dorsal Premotor Cortex Exerts State-Dependent Causal Influences on Activity in Contralateral Primary Motor and Dorsal Premotor Cortex. Cerebral Cortex, 2008, 18, 1281-1291.	2.9	173
39	Evaluation of 2D multiband EPI imaging for high-resolution, whole-brain, task-based fMRI studies at 3T: Sensitivity and slice leakage artifacts. NeuroImage, 2016, 124, 32-42.	4.2	170
40	Unified segmentation based correction of R1 brain maps for RF transmit field inhomogeneities (UNICORT). NeuroImage, 2011, 54, 2116-2124.	4.2	168
41	Voxel-based morphometry reveals reduced grey matter volume in the temporal cortex of developmental prosopagnosics. Brain, 2009, 132, 3443-3455.	7.6	166
42	Advances in MRI-based computational neuroanatomy. Current Opinion in Neurology, 2015, 28, 313-322.	3.6	166
43	Improved segmentation of deep brain grey matter structures using magnetization transfer (MT) parameter maps. NeuroImage, 2009, 47, 194-198.	4.2	164
44	hMRI – A toolbox for quantitative MRI in neuroscience and clinical research. NeuroImage, 2019, 194, 191-210.	4.2	161
45	Optimization and validation of methods for mapping of the radiofrequency transmit field at 3T. Magnetic Resonance in Medicine, 2010, 64, 229-238.	3.0	159
46	Optimized EPI for fMRI studies of the orbitofrontal cortex: compensation of susceptibility-induced gradients in the readout direction. Magnetic Resonance Materials in Physics, Biology, and Medicine, 2007, 20, 39-49.	2.0	157
47	Causal evidence for frontal involvement in memory target maintenance by posterior brain areas during distracter interference of visual working memory. Proceedings of the National Academy of Sciences of the United States of America, 2011, 108, 17510-17515.	7.1	157
48	Deep and Superficial Amygdala Nuclei Projections Revealed In Vivo by Probabilistic Tractography. Journal of Neuroscience, 2011, 31, 618-623.	3.6	139
49	Connectivity-based neurofeedback: Dynamic causal modeling for real-time fMRI. NeuroImage, 2013, 81, 422-430.	4.2	135
50	Hemispheric Differences in Frontal and Parietal Influences on Human Occipital Cortex: Direct Confirmation with Concurrent TMS–fMRI. Journal of Cognitive Neuroscience, 2009, 21, 1146-1161.	2.3	133
51	Neuronal mechanisms underlying control of a brain-computer interface. European Journal of Neuroscience, 2005, 21, 3169-3181.	2.6	132
52	Robust and Fast Whole Brain Mapping of the RF Transmit Field B1 at 7T. PLoS ONE, 2012, 7, e32379.	2.5	127
53	Single-shot compensation of image distortions and BOLD contrast optimization using multi-echo EPI for real-time fMRI. NeuroImage, 2005, 24, 1068-1079.	4.2	126
54	MRI in traumatic spinal cord injury: from clinical assessment to neuroimaging biomarkers. Lancet Neurology, The, 2019, 18, 1123-1135.	10.2	125

#	Article	IF	CITATIONS
55	Traumatic and nontraumatic spinal cord injury: pathological insights from neuroimaging. Nature Reviews Neurology, 2019, 15, 718-731.	10.1	125
56	Benign Partial Epilepsy in Childhood: Selective Cognitive Deficits Are Related to the Location of Focal Spikes Determined by Combined EEG/MEG. Epilepsia, 2005, 46, 1661-1667.	5.1	121
57	The Kuleshov Effect: the influence of contextual framing on emotional attributions. Social Cognitive and Affective Neuroscience, 2006, 1, 95-106.	3.0	116
58	The habenula encodes negative motivational value associated with primary punishment in humans. Proceedings of the National Academy of Sciences of the United States of America, 2014, 111, 11858-11863.	7.1	116
59	Quantitative magnetic resonance imaging of brain anatomy and in vivo histology. Nature Reviews Physics, 2021, 3, 570-588.	26.6	115
60	Improving Visual Perception through Neurofeedback. Journal of Neuroscience, 2012, 32, 17830-17841.	3.6	113
61	Mismatch Negativity Responses in Schizophrenia: A Combined fMRI and Whole-Head MEG Study. American Journal of Psychiatry, 2004, 161, 294-304.	7.2	106
62	Interhemispheric Effect of Parietal TMS on Somatosensory Response Confirmed Directly with Concurrent TMS–fMRI. Journal of Neuroscience, 2008, 28, 13202-13208.	3.6	106
63	Specific white matter tissue microstructure changes associated with obesity. NeuroImage, 2016, 125, 36-44.	4.2	106
64	Locus coeruleus integrity in old age is selectively related to memories linked with salient negative events. Proceedings of the National Academy of Sciences of the United States of America, 2018, 115, 2228-2233.	7.1	104
65	Microstructural imaging of human neocortex in vivo. NeuroImage, 2018, 182, 184-206.	4.2	101
66	Whole-Brain In-vivo Measurements of the Axonal G-Ratio in a Group of 37 Healthy Volunteers. Frontiers in Neuroscience, 2015, 9, 441.	2.8	97
67	Manipulating motor performance and memory through real-time fMRI neurofeedback. Biological Psychology, 2015, 108, 85-97.	2.2	97
68	Progressive neurodegeneration following spinal cord injury. Neurology, 2018, 90, e1257-e1266.	1.1	97
69	Highâ€resolution functional MRI at 3 T: 3D/2D echoâ€planar imaging with optimized physiological noise correction. Magnetic Resonance in Medicine, 2013, 69, 1657-1664.	3.0	93
70	A general linear relaxometry model of R ₁ using imaging data. Magnetic Resonance in Medicine, 2015, 73, 1309-1314.	3.0	90
71	fMRI Brain-Computer Interfaces. IEEE Signal Processing Magazine, 2008, 25, 95-106.	5.6	89
72	The human amygdala is sensitive to the valence of pictures and sounds irrespective of arousal: an fMRI study. Social Cognitive and Affective Neuroscience, 2008, 3, 233-243.	3.0	85

#	Article	IF	CITATIONS
73	Dynamic causal modeling: A generative model of slice timing in fMRI. NeuroImage, 2007, 34, 1487-1496.	4.2	84
74	An evaluation of prospective motion correction (PMC) for high resolution quantitative MRI. Frontiers in Neuroscience, 2015, 9, 97.	2.8	84
75	In-vivo magnetic resonance imaging (MRI) of laminae in the human cortex. Neurolmage, 2019, 197, 707-715.	4.2	83
76	Dissociable roles of human inferior frontal gyrus during action execution and observation. NeuroImage, 2012, 60, 1671-1677.	4.2	82
77	Brain tissue properties differentiate between motor and limbic basal ganglia circuits. Human Brain Mapping, 2014, 35, 5083-5092.	3.6	82
78	Mismatch responses to randomized gradient switching noise as reflected by fMRI and whole-head magnetoencephalography. Human Brain Mapping, 2002, 16, 190-195.	3.6	81
79	Choking on the Money. Psychological Science, 2009, 20, 955-962.	3.3	81
80	Developing 3D microscopy with CLARITY on human brain tissue: Towards a tool for informing and validating MRI-based histology. NeuroImage, 2018, 182, 417-428.	4.2	81
81	Tracking sensory system atrophy and outcome prediction in spinal cord injury. Annals of Neurology, 2015, 78, 751-761.	5.3	77
82	Multi-voxel pattern analysis in human hippocampal subfields. Frontiers in Human Neuroscience, 2012, 6, 290.	2.0	74
83	A Stable Sparse Fear Memory Trace in Human Amygdala. Journal of Neuroscience, 2011, 31, 9383-9389.	3.6	73
84	Quantitative MRI provides markers of intra-, inter-regional, and age-related differences in young adult cortical microstructure. NeuroImage, 2018, 182, 429-440.	4.2	71
85	Flexible head-casts for high spatial precision MEG. Journal of Neuroscience Methods, 2017, 276, 38-45.	2.5	69
86	Estimating the apparent transverse relaxation time (R2*) from images with different contrasts (ESTATICS) reduces motion artifacts. Frontiers in Neuroscience, 2014, 8, 278.	2.8	68
87	Prospective motion correction of 3D echo-planar imaging data for functional MRI using optical tracking. NeuroImage, 2015, 113, 1-12.	4.2	68
88	Axonal integrity predicts cortical reorganisation following cervical injury. Journal of Neurology, Neurosurgery and Psychiatry, 2012, 83, 629-637.	1.9	65
89	Superficial white matter imaging: Contrast mechanisms and whole-brain in vivo mapping. Science Advances, 2020, 6, .	10.3	65
90	Generic acquisition protocol for quantitative MRI of the spinal cord. Nature Protocols, 2021, 16, 4611-4632.	12.0	65

#	Article	IF	CITATIONS
91	An EEG-Driven Brain-Computer Interface Combined With Functional Magnetic Resonance Imaging (fMRI). IEEE Transactions on Biomedical Engineering, 2004, 51, 971-974.	4.2	63
92	Degeneration of the Injured Cervical Cord Is Associated with Remote Changes in Corticospinal Tract Integrity and Upper Limb Impairment. PLoS ONE, 2012, 7, e51729.	2.5	62
93	Decoding representations of scenes in the medial temporal lobes. Hippocampus, 2012, 22, 1143-1153.	1.9	62
94	Efficient fat suppression by sliceâ€selection gradient reversal in twiceâ€refocused diffusion encoding. Magnetic Resonance in Medicine, 2008, 60, 1256-1260.	3.0	60
95	The impact of post-processing on spinal cord diffusion tensor imaging. NeuroImage, 2013, 70, 377-385.	4.2	59
96	Multiparameter mapping of relaxation (<scp>R1</scp> , <scp>R2</scp> *), proton density and magnetization transfer saturation at <scp>3 T</scp> : A multicenter dualâ€vendor reproducibility and repeatability study. Human Brain Mapping, 2020, 41, 4232-4247.	3.6	59
97	Quantitative magnetization transfer in in vivo healthy human skeletal muscle at 3 T. Magnetic Resonance in Medicine, 2010, 64, 1739-1748.	3.0	57
98	Iron Level and Myelin Content in the Ventral Striatum Predict Memory Performance in the Aging Brain. Journal of Neuroscience, 2016, 36, 3552-3558.	3.6	55
99	The quest for the best: The impact of different EPI sequences on the sensitivity of random effect fMRI group analyses. NeuroImage, 2016, 126, 49-59.	4.2	55
100	NODDI-DTI: Estimating Neurite Orientation and Dispersion Parameters from a Diffusion Tensor in Healthy White Matter. Frontiers in Neuroscience, 2017, 11, 720.	2.8	54
101	Voxel-based analysis of grey and white matter degeneration in cervical spondylotic myelopathy. Scientific Reports, 2016, 6, 24636.	3.3	52
102	Image artifacts in concurrent transcranial magnetic stimulation (TMS) and fMRI caused by leakage currents: Modeling and compensation. Journal of Magnetic Resonance Imaging, 2009, 29, 1211-1217.	3.4	48
103	Motor phenotype and magnetic resonance measures of basal ganglia iron levels in Parkinson's disease. Parkinsonism and Related Disorders, 2013, 19, 1136-1142.	2.2	48
104	A novel coil array for combined TMS/fMRI experiments at 3 T. Magnetic Resonance in Medicine, 2015, 74, 1492-1501.	3.0	46
105	Quantitative MRI of rostral spinal cord and brain regions is predictive of functional recovery in acute spinal cord injury. NeuroImage: Clinical, 2018, 20, 556-563.	2.7	46
106	Functional Sensitivity of 2D Simultaneous Multi-Slice Echo-Planar Imaging: Effects of Acceleration on g-factor and Physiological Noise. Frontiers in Neuroscience, 2017, 11, 158.	2.8	45
107	Motor Affordance and its Role for Visual Working Memory: Evidence from fMRI studies. Experimental Psychology, 2004, 51, 258-269.	0.7	45
108	Dorsal and ventral horn atrophy is associated with clinical outcome after spinal cord injury. Neurology, 2018, 90, e1510-e1522.	1.1	44

#	Article	IF	CITATIONS
109	When the Brain Takes â€~BOLD' Steps: Real-Time fMRI Neurofeedback Can Further Enhance the Ability to Gradually Self-regulate Regional Brain Activation. Neuroscience, 2018, 378, 71-88.	2.3	42
110	Direct Evidence for Attention-Dependent Influences of the Frontal Eye-Fields on Feature-Responsive Visual Cortex. Cerebral Cortex, 2014, 24, 2815-2821.	2.9	41
111	Correction of vibration artifacts in DTI using phaseâ€encoding reversal (COVIPER). Magnetic Resonance in Medicine, 2012, 68, 882-889.	3.0	40
112	Mapping Short Association Fibers in the Early Cortical Visual Processing Stream Using In Vivo Diffusion Tractography. Cerebral Cortex, 2020, 30, 4496-4514.	2.9	40
113	Embodied neurology: an integrative framework for neurological disorders. Brain, 2016, 139, 1855-1861.	7.6	39
114	Rapid radiofrequency field mapping in vivo using singleâ€ s hot STEAM MRI. Magnetic Resonance in Medicine, 2008, 60, 739-743.	3.0	38
115	Using High Angular Resolution Diffusion Imaging Data to Discriminate Cortical Regions. PLoS ONE, 2013, 8, e63842.	2.5	37
116	A method for improving the performance of gradient systems for diffusion-weighted MRI. Magnetic Resonance in Medicine, 2007, 58, 763-768.	3.0	34
117	Method for simultaneous voxelâ€based morphometry of the brain and cervical spinal cord area measurements using 3Dâ€MDEFT. Journal of Magnetic Resonance Imaging, 2010, 32, 1242-1247.	3.4	33
118	The effect of local perturbation fields on human DTI: Characterisation, measurement and correction. NeuroImage, 2012, 60, 562-570.	4.2	33
119	Vascular autorescaling of fMRI (VasA fMRI) improves sensitivity of population studies: A pilot study. NeuroImage, 2016, 124, 794-805.	4.2	33
120	Stimulating neural plasticity with realâ€ŧime f <scp>MRI</scp> neurofeedback in <scp>H</scp> untington's disease: A proof of concept study. Human Brain Mapping, 2018, 39, 1339-1353.	3.6	33
121	A unified 3D map of microscopic architecture and MRI of the human brain. Science Advances, 2022, 8, eabj7892.	10.3	33
122	Retrospective correction of physiological noise in DTI using an extended tensor model and peripheral measurements. Magnetic Resonance in Medicine, 2013, 70, 358-369.	3.0	32
123	Cognitive enhancement through real-time fMRI neurofeedback. Current Opinion in Behavioral Sciences, 2015, 4, 122-127.	3.9	32
124	fMRI protocol optimization for simultaneously studying small subcortical and cortical areas at 7Â T. NeuroImage, 2020, 219, 116992.	4.2	32
125	Identification of signal bias in the variable flip angle method by linear display of the algebraic ernst equation. Magnetic Resonance in Medicine, 2011, 66, 669-677.	3.0	31
126	The traveling heads 2.0: Multicenter reproducibility of quantitative imaging methods at 7 Tesla. NeuroImage, 2021, 232, 117910.	4.2	31

#	Article	IF	CITATIONS
127	Correction of interâ€scan motion artifacts in quantitative R1 mapping by accounting for receive coil sensitivity effects. Magnetic Resonance in Medicine, 2016, 76, 1478-1485.	3.0	30
128	The variability of MR axon radii estimates in the human white matter. Human Brain Mapping, 2021, 42, 2201-2213.	3.6	30
129	In vivo evidence of remote neural degeneration in the lumbar enlargement after cervical injury. Neurology, 2019, 92, e1367-e1377.	1.1	29
130	Measuring the iron content of dopaminergic neurons in substantia nigra with MRI relaxometry. NeuroImage, 2021, 239, 118255.	4.2	28
131	Can we predict realâ€ŧime <scp>fMRI</scp> neurofeedback learning success from pretraining brain activity?. Human Brain Mapping, 2020, 41, 3839-3854.	3.6	27
132	Open-access quantitative MRI data of the spinal cord and reproducibility across participants, sites and manufacturers. Scientific Data, 2021, 8, 219.	5.3	27
133	Real-time functional magnetic imaging—brain–computer interface and virtual reality. Progress in Brain Research, 2011, 192, 263-272.	1.4	26
134	Synthetic quantitative MRI through relaxometry modelling. NMR in Biomedicine, 2016, 29, 1729-1738.	2.8	25
135	Example dataset for the hMRI toolbox. Data in Brief, 2019, 25, 104132.	1.0	24
136	Structure predicts function: Combining non-invasive electrophysiology with in-vivo histology. Neurolmage, 2015, 108, 377-385.	4.2	23
137	Connectivity Changes Underlying Neurofeedback Training of Visual Cortex Activity. PLoS ONE, 2014, 9, e91090.	2.5	22
138	High-resolution diffusion kurtosis imaging at 3T enabled by advanced post-processing. Frontiers in Neuroscience, 2014, 8, 427.	2.8	22
139	Predictors of real-time fMRI neurofeedback performance and improvement – A machine learning mega-analysis. NeuroImage, 2021, 237, 118207.	4.2	22
140	7 Tesla MRI Followed by Histological 3D Reconstructions in Whole-Brain Specimens. Frontiers in Neuroanatomy, 2020, 14, 536838.	1.7	21
141	Hyperelastic Susceptibility Artifact Correction of DTI in SPM. Informatik Aktuell, 2013, , 344-349.	0.6	21
142	Infrared oculography—validation of a new method to monitor startle eyeblink amplitudes during fMRI. NeuroImage, 2004, 22, 767-770.	4.2	20
143	Processing of inconsistent emotional information: an fMRI study. Experimental Brain Research, 2008, 186, 401-407.	1.5	20
144	Improved shimming for fMRI specifically optimizing the local BOLD sensitivity. NeuroImage, 2010, 49, 327-336.	4.2	20

#	Article	IF	CITATIONS
145	Longitudinal changes of spinal cord grey and white matter following spinal cord injury. Journal of Neurology, Neurosurgery and Psychiatry, 2021, 92, 1222-1230.	1.9	20
146	Graph-partitioned spatial priors for functional magnetic resonance images. NeuroImage, 2008, 43, 694-707.	4.2	18
147	Phase informed model for motion and susceptibility. Human Brain Mapping, 2013, 34, 3086-3100.	3.6	18
148	Mapping the human connectome using diffusion MRI at 300 mT/m gradient strength: Methodological advances and scientific impact. NeuroImage, 2022, 254, 118958.	4.2	18
149	Maximising BOLD sensitivity through automated EPI protocol optimisation. NeuroImage, 2019, 189, 159-170.	4.2	17
150	Relating quantitative <scp>7T MRI</scp> across cortical depths to cytoarchitectonics, gene expression and connectomics. Human Brain Mapping, 2021, 42, 4996-5009.	3.6	17
151	Perceived and mentally rotated contents are differentially represented in cortical depth of V1. Communications Biology, 2021, 4, 1069.	4.4	17
152	A comprehensive approach for correcting voxelâ€wise bâ€value errors in diffusion MRI. Magnetic Resonance in Medicine, 2020, 83, 2173-2184.	3.0	15
153	Local striatal reward signals can be predicted from corticostriatal connectivity. NeuroImage, 2017, 159, 9-17.	4.2	15
154	Brain iron content in systemic iron overload: A beta-thalassemia quantitative MRI study. NeuroImage: Clinical, 2019, 24, 102058.	2.7	14
155	POAS4SPM: A Toolbox for SPM to Denoise Diffusion MRI Data. Neuroinformatics, 2015, 13, 19-29.	2.8	12
156	Real-time decoding of covert attention in higher-order visual areas. NeuroImage, 2018, 169, 462-472.	4.2	12
157	Melody Processing Characterizes Functional Neuroanatomy in the Aging Brain. Frontiers in Neuroscience, 2018, 12, 815.	2.8	12
158	Flexible proton density (PD) mapping using multi-contrast variable flip angle (VFA) data. NeuroImage, 2019, 186, 464-475.	4.2	12
159	Combining navigator and optical prospective motion correction for <scp>highâ€quality</scp> 500 μm resolution quantitative <scp>multiâ€parameter</scp> mapping at <scp>7T</scp> . Magnetic Resonance in Medicine, 2022, 88, 787-801.	3.0	12
160	Microstructural parameter estimation in vivo using diffusion MRI and structured prior information. Magnetic Resonance in Medicine, 2016, 75, 1787-1796.	3.0	11
161	Safety of Tattoos in Persons Undergoing MRI. New England Journal of Medicine, 2019, 380, 495-496.	27.0	11
162	Optimizing Data for Modeling Neuronal Responses. Frontiers in Neuroscience, 2018, 12, 986.	2.8	11

#	Article	IF	CITATIONS
163	PyRates—A Python framework for rate-based neural simulations. PLoS ONE, 2019, 14, e0225900.	2.5	11
164	Midbrain fMRI: Applications, Limitations and Challenges. Biological Magnetic Resonance, 2015, , 581-609.	0.4	11
165	Biophysically motivated efficient estimation of the spatially isotropic component from a single gradientâ€recalled echo measurement. Magnetic Resonance in Medicine, 2019, 82, 1804-1811.	3.0	10
166	Activity or connectivity? A randomized controlled feasibility study evaluating neurofeedback training in Huntington's disease. Brain Communications, 2020, 2, fcaa049.	3.3	10
167	Microstructural plasticity in nociceptive pathways after spinal cord injury. Journal of Neurology, Neurosurgery and Psychiatry, 2021, 92, 863-871.	1.9	10
168	Modelling Temporal Stability of EPI Time Series Using Magnitude Images Acquired with Multi-Channel Receiver Coils. PLoS ONE, 2012, 7, e52075.	2.5	9
169	Objective Bayesian fMRI analysisââ,¬â€a pilot study in different clinical environments. Frontiers in Neuroscience, 2015, 9, 168.	2.8	8
170	Acquisition of sensorimotor fMRI under general anaesthesia: Assessment of feasibility, the BOLD response and clinical utility. NeuroImage: Clinical, 2019, 23, 101923.	2.7	8
171	Physiological basis of vascular autocalibration (Vas <scp>A</scp>): Comparison to hypercapnia calibration methods. Magnetic Resonance in Medicine, 2017, 78, 1168-1173.	3.0	7
172	Author response: Progressive neurodegeneration following spinal cord injury: Implications for clinical trials. Neurology, 2018, 91, 985-985.	1.1	7
173	Extrapyramidal plasticity predicts recovery after spinal cord injury. Scientific Reports, 2020, 10, 14102.	3.3	7
174	The relationship between hippocampal-dependent task performance and hippocampal grey matter myelination and iron content. Brain and Neuroscience Advances, 2021, 5, 239821282110119.	3.4	7
175	Finding the best clearing approach - Towards 3D wide-scale multimodal imaging of aged human brain tissue. NeuroImage, 2022, 247, 118832.	4.2	7
176	Reliability of quantitative multiparameter maps is high for magnetization transfer and proton density but attenuated for <scp>R₁</scp> and <scp>R₂</scp> * in healthy young adults. Human Brain Mapping, 2022, 43, 3585-3603.	3.6	6
177	Tx/Rx Head Coil Induces Less RF Transmit-Related Heating than Body Coil in Conductive Metallic Objects Outside the Active Area of the Head Coil. Frontiers in Neuroscience, 2017, 11, 15.	2.8	5
178	A group-level comparison of volumetric and combined volumetric-surface normalization for whole brain analyses of myelin and iron maps. Magnetic Resonance Imaging, 2018, 54, 225-240.	1.8	5
179	Spatial gradients of healthy aging: a study of myelin-sensitive maps. Neurobiology of Aging, 2019, 79, 83-92.	3.1	5
180	Modeling radio-frequency energy-induced heating due to the presence of transcranial electric stimulation setup at 3T. Magnetic Resonance Materials in Physics, Biology, and Medicine, 2020, 33, 793-807.	2.0	5

#	Article	IF	CITATIONS
181	Reducing Susceptibility Distortion Related Image Blurring in Diffusion MRI EPI Data. Frontiers in Neuroscience, 2021, 15, 706473.	2.8	5
182	Orthogonalizing crusher and diffusionâ€encoding gradients to suppress undesired echo pathways in the twiceâ€refocused spin echo diffusion sequence. Magnetic Resonance in Medicine, 2014, 71, 506-515.	3.0	4
183	Combining Deep Learning and Active Contours Opens The Way to Robust, Automated Analysis of Brain Cytoarchitectonics. Lecture Notes in Computer Science, 2018, , 179-187.	1.3	4
184	Simulating Local Deformations in the Human Cortex Due to Blood Flow-Induced Changes in Mechanical Tissue Properties: Impact on Functional Magnetic Resonance Imaging. Frontiers in Neuroscience, 2021, 15, 722366.	2.8	3
185	Multiâ€parameter quantitative mapping of R1, R2*, PD, and MTsat is reproducible when accelerated with Compressed SENSE. NeuroImage, 2022, 253, 119092.	4.2	3
186	A new method for joint susceptibility artefact correction and super-resolution for dMRI. , 2014, , .		2
187	Volitional modulation of higher-order visual cortex alters human perception. Neurolmage, 2019, 188, 291-301.	4.2	2
188	Towards a representative reference for MRI-based human axon radius assessment using light microscopy. Neurolmage, 2022, 249, 118906.	4.2	2
189	Modeling Electromagnetic Exposure in Humans Inside a Whole-Body Birdcage Coil Excited by a Two-Channel Parallel Transmitter Operated at 123 MHz. IEEE Journal of Electromagnetics, RF and Microwaves in Medicine and Biology, 2020, 4, 247-253.	3.4	1
190	A brief history of real-time fMRI neurofeedback. , 2021, , 1-19.		1
191	Identifying Intracortical Partial Voluming Effects Using Cortical Surface Normals in Quantitative MRI T1 Maps Sensitive to Microstructure. Informatik Aktuell, 2016, , 14-19.	0.6	0

192 Echtzeit-fMRT. , 2013, , 103-117.

0